Proceedings of 12th Cambridge Workshop on Cool Stars, Stellar Systems, & The Sun, 2003 University of Colorado.

Coronal Variability in the Young Cluster NGC 2516

Scott J. Wolk[1], F.R. Harnden Jr.[1], S.S. Murray[1], N.R. Adams[1], F. Damiani[2], E. Flaccomio[2], G. Micela[2], S. Sciortino[2], R. Jeffries[3]

Abstract.
We discuss our ongoing analysis of *Chandra* observations of the young open cluster NGC 2516. NGC 2516 was observed by *Chandra* to boresight correct the spacecraft's focal plane instruments. Because of this, CXO observed NGC 2516 with all imaging arrangements available. In addition, it has been observed as part of the HRC guaranteed time program and is scheduled for return boresight calibration visits. This makes it the best cluster to study for long term variability. NGC 2516 is about 100 Myrs old and less than 400 pc away. We have detected about 275 sources, almost half of which have been confirmed as cluster members. We explore techniques of combining ACIS and HRC *Chandra* data for timing analysis. We have been able to combine almost 100 ks of observation time, spread over four epochs to study variability in this cluster on multiple time scales.

1. Introduction

Sometimes referred to as the "Southern Pleiades", NGC 2516 is about 141 Myrs old (Meynet et al. 1993) and less than 400 pc away (390pc; Jeffries et al. 1997). It occupies an interesting place in the evolutionary time sequence, somewhat older than the Pleiades, yet younger than the Hyades. Its most striking feature is its reported low metalicity, [Fe/H]=-0.32 $\pm$ 0.06 (Jeffries 1997, in agreement with Cameron 1985). The significance of metalicity in coronal activity was examined by Micela et al. (2000). Using the ROSAT HRI they compared NGC 2516 with the Pleiades and concluded that the peak of the dM star X-ray luminosity level does not depend on metalicity. This suggests that the activity level for dM stars is insensitive to a change of a factor of two in stellar metalicity.

NGC 2516 is a unique cluster from *Chandra's* point of view because it was observed to boresight correct the spacecraft's focal plane instruments. Because of this, NGC 2516 was observed with all four imaging arrangements available to *Chandra*. In addition, it has been observed as part of the HRC guaranteed time program and has made a return boresight calibration visits. In all, there have been eight successful observations of NGC 2516 spaced over about 19 months. This makes it the best cluster to study for long term variability.

---

[1]Harvard–Smithsonian Center for Astrophysics

[2]Osservatorio Astronomico di Palermo G.S. Vaiana

[3]Department of Physics, Keele University

In our first *Chandra*-based study of this cluster (Harnden et al. 2001), we examined only the calibration data for the HRC-I and ACIS-I detectors. We detected about 150 sources, 42% of which have been confirmed as cluster members. G and K stars in NGC 2516 were found to be less X-ray luminous than the G and K Pleiades stars while the median log L_X value for NGC 2516 F-type stars is higher than that of the Pleiades.

2. Observations & Reductions

The observations of NGC 2516 taken by *Chandra* were highly varied. Each main scientific configuration was used during the first month of the mission. At this time the ACIS focal plane temperature was -90C and the CCDs were suffering serious degradation with each passage through the radiation belts. The quantum efficiency as a function of energy is therefore poorly known and good spectral analysis of those data will be difficult. The ACIS-I/S observations were broken up into two parts separated by a passage through the radiation belt which lasted about 13 hours. Due to a lack of sources in the ACIS-S image, an ACIS image was taken in the with ACIS-S at the aim-point, but chips I2 and I3 were on in place of S0 and S5, this is known as the ACIS-SI configuration. The pointing was slightly offset for this observation and the focal plane was at -100C.

Both HRC-S observations of NGC 2516 were dominated by UV light from B stars. The UV filtering is of various thicknesses on the HRC-S to facilitate the use of the low energy grating. The result was expected and usable for the boresight, but not for X-ray science. The first two HRC-I observations were made without the HRC fully translated into the focal plane. Few focused X-ray events were seen. HRC-I did successfully observe the cluster, and has returned twice more with separations of about 6 months and 18 months from the original observation.

All data have been processed via CXCDS pipeline processing, with R4CU5 or later. All status flags, energy corrections, and bad pixel and column masks used were similar. Our time series analysis code preferred to handle data which was temporally continuous so the original standard processing data was used on a per obsid basis.

3. Creation of Light–Curves

In our previous light-curve studies (of M42; Sciortino et al. 2000), we created a light-curve by extracting the photon arrival times within a given aperture using simple IDL based tools. In this study we discovered almost immediately that the background was highly variable. Therefore we needed to apply more sophisticated techniques and settled on new functionality in the CIAO tool DMEXTRACT. As of CIAO 2.1, DMEXTRACT can extract a time histogram of a source. As of CIAO 2.2, this time histogram can be background subtracted.

For the background we created a "swiss cheese" background image by removing all the sources detected in each observation using DMCOPY. We chose an aperture of three times the radius determined by the PWDETECT (Damiani et al. 2001; see also $http://www.astropa.unipa.it/progetti\_ricerca/PWDetect$) algorithm which should have included over 90% of the energy from each source.

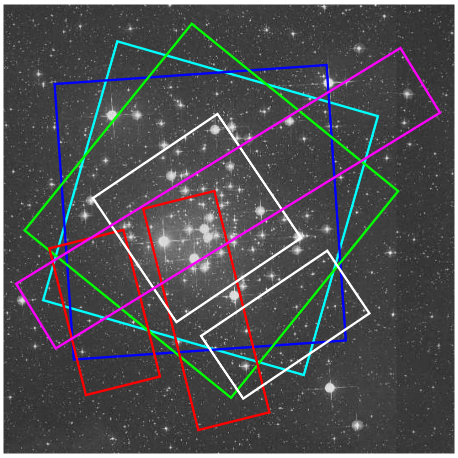

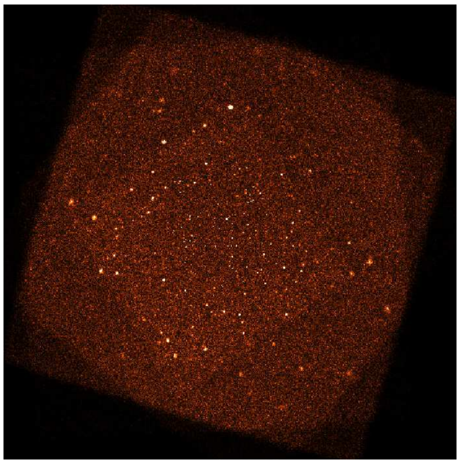

Figure 1. The image on the left shows the eight X-ray observations overlaid on a DSS image of NGC2516. The ACIS-I (white) and ACIS-S (magenta) fields were observed twice using identical pointings. The image on the right is an X-ray composite image created by combining the 3 HRC exposures with the 2 ACIS I exposures (I-array only). In both figures, North is up, East is to the left.

Background maps were made for each of the HRC exposures. Two background maps were made for the ACIS exposures, one for the front illuminated chips, one for the back illuminated chips. We discovered 2 features in the region library during this process: When many small regions are removed from a large region, the total area as reported by the data model increases instead of decreasing. Also the syntax is very sensitive to the ordering of the regions. These issues have been reported. The error caused is of order 1% for the HRC data but may reach 10% in the case of the ACIS data.

We chose an extraction time of 500 seconds as a compromise between having good signal per bin for most of the bright sources, and having sufficient resolution to detect flares of about 2000 seconds in length.

To verify the validity of the background extraction, a $45''$ region devoid of sources near the aimpoint was selected as a background comparison region. As shown in Figure 2, the “swiss cheese” background correction worked quite well. The residual in the ACIS-I and HRC-I image had an absolute value of less than 0.3 counts/500 second/$45''$. The residual of the back illuminated ACIS chips was a bit higher: about 16 counts/500 sec/$45''$. This elevated residual is under investigation. However, it is reasonably flat. DMEXTARCT was run separately for each source and each obsid, with the appropriate background, a total of 2,200 extractions. Data were binned to produce net counts per 500 seconds. The extractions from like detectors were pruned by removing the bins in the early and late parts of each observation which were not indicative of a full 500 second good time interval and then attached. The key data were bin number, bin_start, bin_stop and net_counts per bin. The result was 759 light-curves, 266 for 69 ksec of HRC-I, 148 for 20 ksec for ACIS-S, 211 for 20 ksec of ACIS-I and 134 light-curves for the 10 ksec ACIS-SI observation.

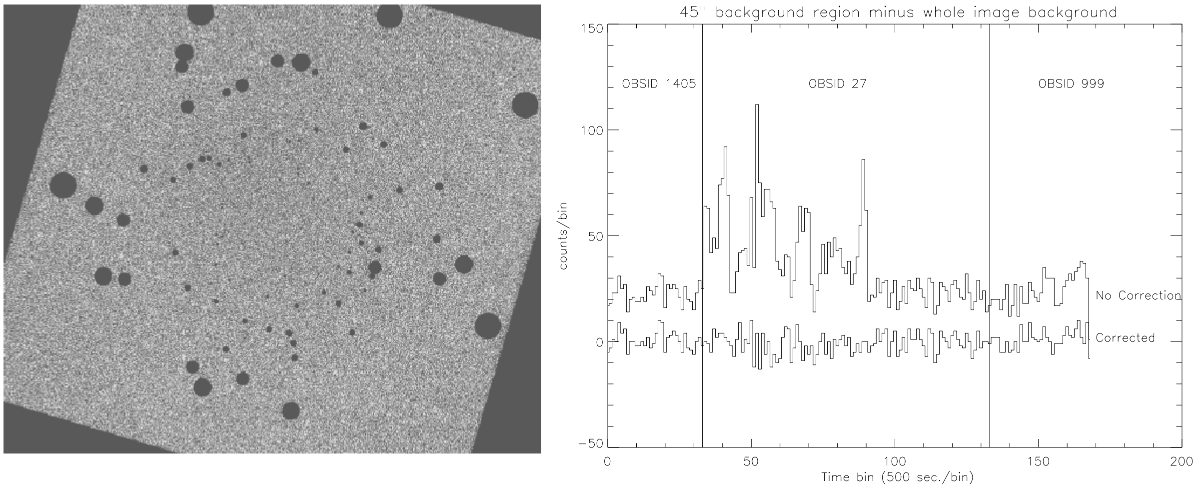

Figure 2. (Left) A "swiss cheese" background map for the HRC (obsid 27) produced by removing all sources detected in this obsid. (Right) A test of the effectiveness of this method. The upper curve represents the count rate in a 45″ diameter region. The lower curve in the result of subtracting the "swiss cheese" background from the background region. Temporal effects cancel well, HRC and ACIS-I residuals are $<$ 0.3 counts/bin. ACIS-S has a significant residual.

4. Variability Analysis

In some cases, particularly the striking flare of at the top of Figure 3, the existence of variability and the nature of the variability is quite easy to assess. However most situations are far less clear cut. We seek a systematic methodology for determining variability and the nature of variability. We chose to address this quantitatively by answering three questions: 1) Is the source constant? 2) Does the source flare? 3) Does the flux level change between visits?

4.1. Question 1: is the source constant?

The one–sample Kolmogorov–Smirnov test determines whether the observed population is drawn from a functional form. In the case of a non-variable object the functional form is a constant photon arrival rate. However, our data were time binned in order to properly subtract out times of high background. To simulate the effective photon arrival times the events in each bin were "spread–out" throughout the bin as though they had arrived uniformly, within the bin. For example, if a bin had 4 events, they were assigned times of bin_start + (1/8)*500., bin_start + (3/8)*500., bin_start + 5/8)*500. and bin_start + (7/8)*500., respectively. This is an approximation to the actual photon arrival times and should result in a systematically higher probability of finding a light–curve compatable with being constant.

One could directly test the time histogram using a two–sample Kolmogorov-Smirnov test. A two–sample Kolmogorov-Smirnov test examines whether the observed population can be derived from the hypothesized population. In the case of these light–curves, the simple non-variable object hypothesis is that the count rate per 500 second bin is a Poisson distribution about a mean. Here the Poisson distribution mean is the same as the mean of the light curve. A better hypothesis is that the observed light-curve is the result of constant source plus Poisson noise sitting on a constant background plus Poisson noise. A constant background is then subtracted. The background is properly scaled for the aperture.

We conducted one and two–sample Kolmogorov-Smirnov test against each source detected by each instrument configuration with over 25 counts. All sources found to be non-constant with 99% confidence were flagged as variable sources. In all cases, the one–sample Kolmogorov-Smirnov test detected less variable sources than the two–sample Kolmogorov-Smirnov test, by about 50%. Since the one–sample test seemed more conservative we chose it as our primary test of variability.

4.2. Question 2: Does the source flare?

X-ray variability of stellar coronae takes many forms. Sometimes flux shows a steady rise or decline, sometimes the flux simply varies much more wildly than expected by Poisson statistics and sometimes there is a dramatic peak in the flux followed by a return to the original level. This last case is known as a flare. To search for flares within our data we adopted the technique of Stelzer et al. (2000). We looked for periods in which data from 3 successive bins (15 minutes), exceeded the mean flux by more than 5 sigma.

4.3. Question 3: Does the change quiescent level?

The most unique feature of this data set with respect to other *Chandra* data sets of young clusters is the number of visits, eight. Each visit was at least 10 kiloseconds so there are good statistics for many of the sources. Unfortunately, the count rate among the different detectors cannot easily be compared because the rates depend on the effective areas. This issue is further complicated by the spectral sensitivity differences among the detectors. We calculated the mean count rate for each source with more than 25 counts in each observation. The count rates are compared among like detector configurations. Finally, we identify all sources which varied by more than three sigma as stars with shifts in their quiescent level. Less than 10% of sources were seen to vary in this way.

5. Results

We cross–correlated our results on variability with the recent catalog by Jeffries et al. (JTH;2001) to better interpret our data. Our findings are summarized in Tables 1 through 3. Fundamentally, 28% of the 275 source detected are found to be variable to 99% confidence using the one–sample KS test. About 12% of the objects were found to flare. The percentages increase somewhat when we limit ourselves to sources which had an X–ray flux of over 2.5 counts/ksec in at least one of the observing windows. We interpret this as the improved photon signal allows greater confidence in the results of the KS statistic.

In Table 1, members and non-members are determined by the colors in the JTH Catalog. Forty–seven percent of the detected sources are cluster members based on their colors. Sixteen percent of the detected sources are probably not cluster members based on their colors (although this estimate may be high since the membership criteria used in JTH was very conservative). The group of non–members includes a few faint blue objects which may be extragalactic in nature. The others may be field stars as NGC 2516 is close to the Gould Belt. These stars seem variable and flare at higher rates than the cluster members.

The remaining 36% of the X-ray sources are nominally unknown since they were photometricly undetected in a survey which was complete past V=20. The unidentified sources are *very* likely extragalactic sources. At our sensitivities, the resulting F_x/F_v ratios are too high to be of stellar nature The next question is why are extragalactic sources so numerous? Giacconi et al. find N(>S) = 370 $(S/2\times10^{-15})^{-.85}$ sources (AGN) degree^{-2} in the *Chandra* Deep Field South. Our total field coverage is a little over 0.25 degree^{-2}, because the three HRC fields are rolled with respect to each other. Our deepest single exposure reached about 2.8×10^{-15} although most only went half as deep and the limiting sensitivity is a function of off-axis angle. Most of the area is at large off-axis distance where the limiting sensitivity is worst. In the end, we estimate between 45 and 90 extragalactic sources within our field. While 100 extragalactic sources is not unreasonable, perhaps there is an additional non–extragalactic population such as embedded sources.

Table 1. Computed Variability

	All Sources			X–ray Bright Only		
	#	Variable	Flare	#	Variable	Flare
members	130	26%	36%	100	32%	13%
non-members	45	42%	38%	34	56%	20%
unknown (V>20?)	100	23%	10%	61	36%	15%
total	275	28%	12%	200	37%	15%

In Table 2, we focus on the effect of segregating the results of the variability analysis by spectral type. In general, the later spectral types show more variability. Especially pronounced is the flare rate of M stars which is about twice the rate of any other sub-group. While not a surprising result, it is true for M stars which are *not* cluster members as well as those which are. Further, the overall variability rate among M stars is no higher than that of other groups.

A real surprise is found among the G stars. While the non-member G stars show variability similar to that of the whole group, G star members showed variability at better than twice the rate of other stars. Perhaps this is an issue of a statistical fluctuation. It is hard to estimate a good error statistic. However, for the G stars we would expect 38% of 12 (4.5) stars to be variable if the G stars are drawn from the general sample of cluster members. The 1σ fluctuation (on 4.5) is 2.1. We observed nine member G stars variables. This appears significant at greater than the 2σ level.

The issue of why the G stars should be bright not at all clear. Youth is an obvious suspect, but this is a flux limited survey, in such a survey one usually selects the more active and/or younger stars. Harnden et al (2001) evaluated the number of "normal coronal source" to be small (∼3), but NGC 2516 is near the Gould Belt so, it is possible that a fraction of the non-members belong to the Gould Belt (previously noted by Harnden et al, Micela et al. 2000, Sciortino et al. 2001). If this is the case a non–negligible fraction of dG non-members are as young (or even younger) of NGC 2516 members at a somewhat larger distance than NGC 2516 and with a higher activity level.

Table 2. Variability as a Function of Spectral Color

Sp. Type	#	Obstime*	% Flared	% Variable
B	1	90.0	0%	100%
A	15	998.5	13%	27%
F	33	2382.0	6%	27%
G	22	1419.0	5%	50%
K	60	5201.5	8%	37%
M	54	4570.0	20%	27%
unknown	100	8171.0	10%	28%
total	285**	22,832.0	11%	32%

*Obstime is the sum of the number of stars of a given type observed times the amount of observing time for each star. Units are megaseconds.

**Total is 10 greater than 275 because 10 stars were classified differently by B-V and V-I spectral type determinations.

In the final table, we assay X-ray variability of stars with over 2.5 counts/ksec in at least one observation versus multiplicity as determined by the photometric data in JTH. While flare rates are nearly identical for single stars as for multiples, binaries show slightly enhance levels of variability. This effect is most extreme among the F stars, while the effect is barely noticeable among the M stars.

6. Comparison with M42

We are also in the process of analyzing the *Chandra* GTO observation of M42. The dataset we are working on is a continuous HRC image 63 kiloseconds in duration, obsid 26. The bulk of the data will presented separately (Flaccomio et al 2001, Flaccomio 2001). However it is worthwhile to summarize the results here for comparative purposes. Using similar techniques as those applied to the NGC 2516 datasets, about 745 point sources were detected. Variability is very common as seen in the included movie. Using the one-sample KS test 33% of sources were variable at 90% confidence, 20% were variable at 99% confidence.

Table 3. X-ray Bright Stars Sorted by Photometric Multiplicity

Spectral Type	#	Binaries Variable	Flare	#	Single Stars Variable	Flare
B	0	-	-	1	100%	0%
A	6	33%	17%	5	40%	20%
F	11	55%	9%	17	12%	6%
G	7	71%	0%	11	55%	9%
K	15	53%	7%	34	41%	12%
M	10	40%	30%	29	34%	24%
total	49	59%	12%	97	36%	14%

This latter number is slightly lower than the 26% variability (99% confidence) we report for members of NGC 2516.

The observation of M42 was not subject to the variable background level experienced by some of the noisier HRC measurements. Thus, it is possible that the KS test is detecting the background variations. Further, we do not know of the typical source count statistic is the same or not in the 2 clusters. The observation of Orion was shorter by 50% than the total observing time spent on NGC 2516, so we cannot argue that the variability rate is lower in the young cluster M42 than the 140 Myr old cluster. However, it is clear that the rates are not significantly different. Over the range of the first 140 million years of a stars life, intrinsic variability does not change much.

7. Conclusions

We have been able to successfully extract and background correct 275 light–curves for sources in NGC 2516 and calculated meaningful variability properties for 200. We tested each light–curve for variability and flaring. We find that flare type variability accounts for about 40% of all X-ray variability. Other results include:

- The occurrence of short time scale variability is about 30% which is close to the level observed in the Orion Nebular Cluster.
- Non-cluster members are less constant in flux than cluster members. These are possibly Gould Belt objects.
- M stars flare somewhat more than other stars, independent of membership.
- Changes in the quiescent level, or variability on longer time scales is observed in less than 10% of cases.
- G star members seem over–variable.
- The X–ray flux from multiples tends to be less stable than single stars.

The first, second and third points strongly indicate that variability and flaring are not strong functions of age. Our ability to detect X-rays becomes limited as stars age and their coronal emission lowers. But there is no evidence here that suggests that the relative variability of coronal emission changes with age.

Acknowledgments. This project is supported by the *Chandra* X–ray Center under NASA contract NAS8-39073.

References

Cameron, L.M. 1985, A&A, 147, 39.

Damiani, F. et al. 2001, (in Prep.)

Flaccomio, E. 2001, Ph.D. Thesis.

Flaccomio, E. et al. 2001, *Stellar Coronae in the Chandra and XMM-Newton era, Favata & Drake eds.* submitted.

Giacconi et al. 2001, ApJ, 551, 624.

Harnden et al. 2001, ApJ, 257, L141.

Jeffries, R.D. et al. 1997, A&A, 287, 350.

Jeffries, R.D. et al. 2001, A&A, (submitted:astro-ph/0107097)

Meynet, G. et al. 1993, A&AS, 98, 477.

Micela, G. et al. 2000, A&A, 357, 909.

Sciortino, S. et al. 2000, *X–ray Astronomy 2000, Giacconi, Stella, Serio eds.* in press.

Sciortino, S. et al. 2001, A&A, 365, L259.

Stelzer, B. et al. 2000, A&A, 356, 949.

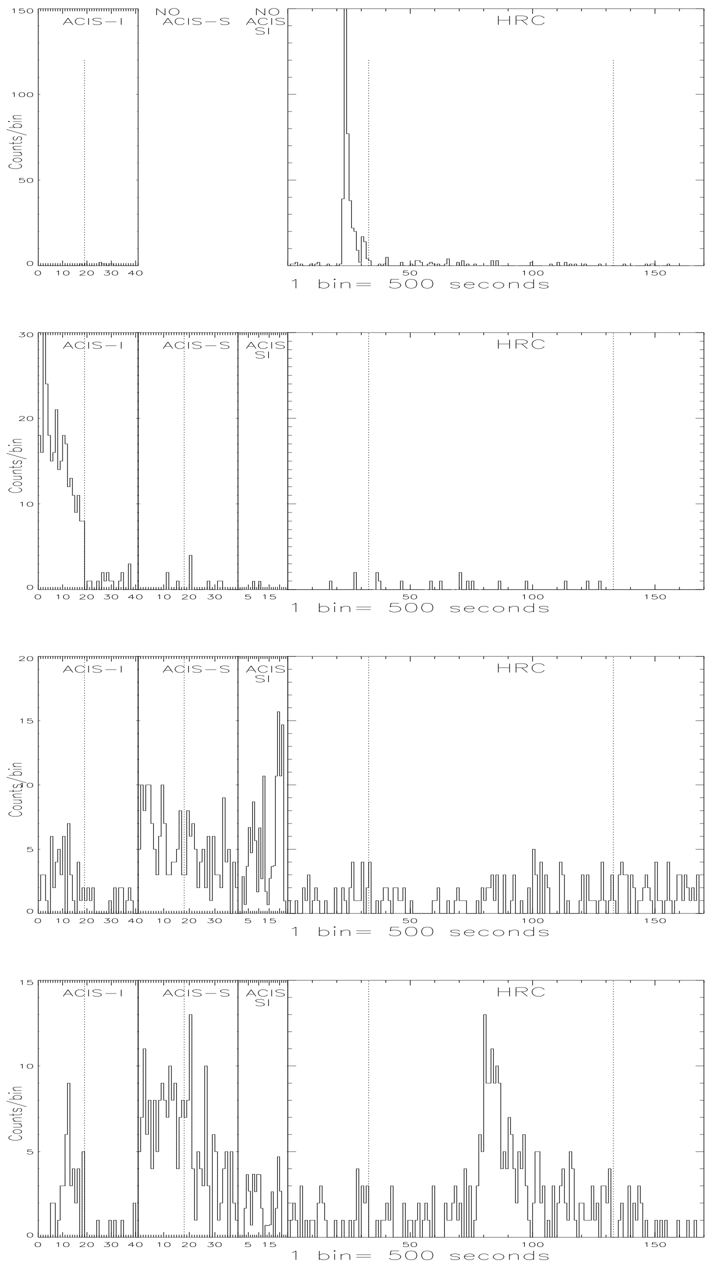

Figure 3. Examples of interesting light–curves. The above light–curves are 85 ksec from start to finish. The top curve has a data gap for the first part because this object lies outside the ACIS field of view. Solid lines indicate a detector change and a gap of between a few days and a few months. The dotted line within any given detector plot indicates a gap as well, in the case of ACIS these gaps are about 13 hours, in the case of HRC these gaps are about 6 months. *One cannot directly compare the count rates among the different detectors due to differences in effective area.*